



LAWRENCE  
LIVERMORE  
NATIONAL  
LABORATORY

# Backscatter measurements for NIF ignition targets

J. D. Moody, P. A. Michel, E. Bond, P. Datte, K. Krauter, S. H. Glenzer, L. Divol, C. Niemann, L. Suter, N. Meezan, B. J. MacGowan, R. Hibbard, R. London, J. Kilkenny, R. Wallace, J. L. Kline, K. Knittel, G. Ross, K. Widmann, J. Jackson, S. Vernon, T. Clancy

May 14, 2010

18th Topical Conference High Temperature Plasma Physics  
Wildwood, NJ, United States  
May 16, 2010 through May 20, 2010

## **Disclaimer**

---

This document was prepared as an account of work sponsored by an agency of the United States government. Neither the United States government nor Lawrence Livermore National Security, LLC, nor any of their employees makes any warranty, expressed or implied, or assumes any legal liability or responsibility for the accuracy, completeness, or usefulness of any information, apparatus, product, or process disclosed, or represents that its use would not infringe privately owned rights. Reference herein to any specific commercial product, process, or service by trade name, trademark, manufacturer, or otherwise does not necessarily constitute or imply its endorsement, recommendation, or favoring by the United States government or Lawrence Livermore National Security, LLC. The views and opinions of authors expressed herein do not necessarily state or reflect those of the United States government or Lawrence Livermore National Security, LLC, and shall not be used for advertising or product endorsement purposes.

## Backscatter measurements for NIF ignition targets

J. D. Moody, P. A. Michel, E. Bond, P. Datte, K. Krauter, S. H. Glenzer,  
L. Divol, C. Niemann[1], L. Sutter, N. Meezan, B. J. MacGowan,  
R. Hibbard, R. London, J. Kilkenny, R. Wallace, J. L. Kline[2],  
K. Knittel, G. Ross, K. Widmann, J. Jackson, S. Vernon, T. Clancy

*Lawrence Livermore National Laboratory,*

*P. O. Box 808, Livermore, CA 94550\**

*[1] Physics Department, University of California*

*Los Angeles, Los Angeles, CA 90095 USA. and*

*[2] Los Alamos National Laboratory, Los Alamos, NM blahblah USA.*

(Dated: May 10, 2010)

## Abstract

Indirect drive ignition targets for use on the National Ignition Facility (NIF) create backscattered light via laser-plasma instabilities (LPI). We have measured the backscatter level in early NIF hohlraum experiments in order to determine the phase-plate and hohlraum material which give the lowest backscattering ( $\leq 10\%$ ) for ignition designs. Backscatter is measured on one inner and one outer beam quad using a suite of detectors. Light scattered into the beam aperture is measured with the FABS (Full Aperture Backscatter System) instrument and light scattered outside the beam aperture is measured with the NBI (Near Backscatter Imager) instrument. Each of these instruments separately measures the stimulated Brillouin (SBS) and stimulated Raman scattered (SRS) light. Both instruments work in conjunction to provide the total backscattered power. The instruments have been constructed to meet temporal resolution, spectral resolution, and amplitude accuracy requirements. In order to achieve the temporally-resolved power accuracy requirement we have added time-resolution capability to the NBI for the first time. This capability provides a temporally resolved spatial image of either SRS or SBS and can be viewed as a movie of the spatially resolved backscatter light distribution. Combining this measurement with the FABS gives the detailed temporal behavior of the backscattered light. We will report on the details of the instruments used to measure backscatter and describe the techniques used to calibrate the system.

PACS numbers: 52.38.-r, 52.25.-b, 52.35.-g

## I. INTRODUCTION

Experiments on the path toward achieving thermonuclear fusion have recently begun[1] on the National Ignition Facility (NIF)[2]. Reaching ignition relies on meeting high performance requirements for both the laser and target. The indirect drive ignition target has a smooth deuterium-tritium ice layer on the inside of a fuel capsule which is suspended in the center of a gold cylinder or hohlraum. Symmetric laser illumination on the inner wall fills the hohlraum with x-rays which ablate the fuel capsule causing it to reach densities and temperatures which initiate nuclear fusion and burn of the fuel[3]. Frequency tripled (351 nm) laser beams provide up to 1.8 MJ of energy to the target with about 10% of this coupled into the fuel capsule[4].

Progress toward ignition requires a strategic set of diagnostic instruments suited to measure the performance of the laser and target. These instruments quantify the characteristics of the incident laser light as well as power loss from the target via scattered light, particles and x-rays. The first series of experiments on indirect drive hohlraum targets has focused on characterizing the energy loss through backscatter light and selecting laser and target properties that limit the total backscatter to less than about 10%.

This paper describes the set of instruments used to make detailed measurements of optical backscattered light from NIF targets. The backscatter diagnostic is divided into three systems which build off of similar instruments installed on other laser systems such as Nova[5], Omega[6, 7], and early light measurements on NIF[8–12].

Figure 1 shows a sketch of the backscatter instrument currently in use on NIF. The instrument consists of three subsystems. The Full Aperture Backscatter System (FABS) measures light backscattered into the full aperture of the incident laser. The FABS provides power time history and temporally resolved spectral measurements of light backscattered into the incident aperture. The Near Backscatter Imaging system (NBI) measures light scattered outside of the FABS aperture and extending out to a cone angle corresponding to about an  $f/4.7$ . A large scatter plate surrounding the incident aperture is mounted inside the target chamber. This plate is viewed with gated ICCD cameras which record 2-D images of the time-integrated light distribution on the scatter plate. A new time-resolved measurement capability has been added to the NBI. This instrument uses 40 optical fibers and an optical streak camera to record the time history of light intensity at many points

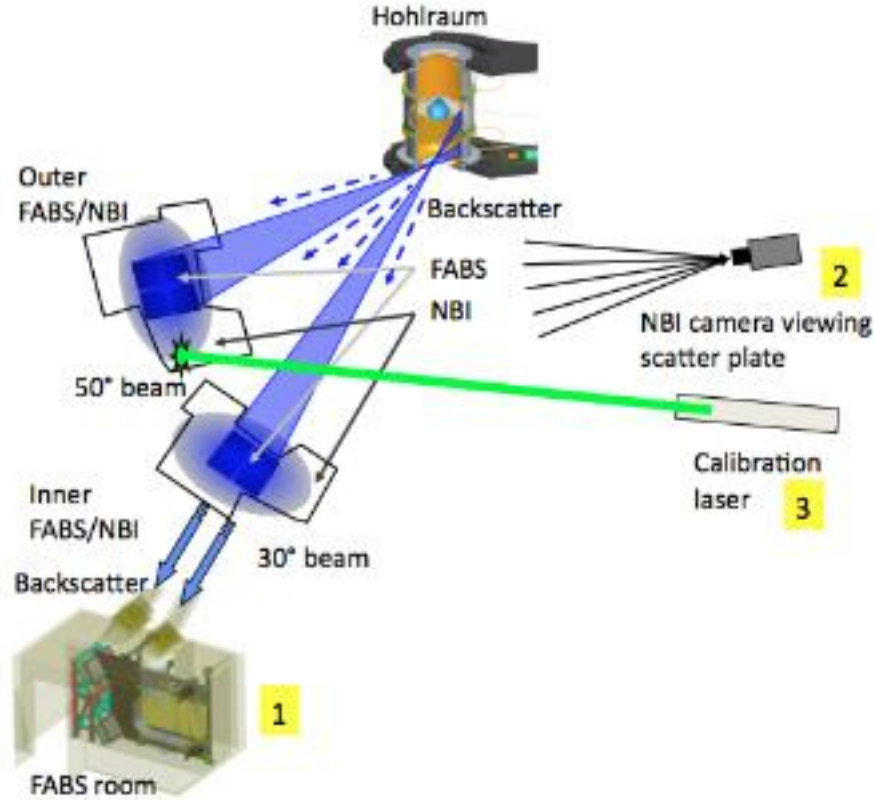


FIG. 1. The backscatter system consists of a 1) FABS instrument and 2) NBI instrument for two NIF quads, and a 3) Pulsed laser calibration instrument.

on the scatter plate. After normalization the data is assembled into a movie showing the evolving light distribution on the scatter plate. This movie contains the quantitative information for determining the complete time-resolved backscatter signal. Both the FABS and NBI systems make separate measurements for light in two independent spectral bands. One band corresponds to the Stimulated Brillouin Scattering (SBS, 350 nm to 353 nm) and the other to Stimulated Raman Scattering (SRS, 450 nm to 750 nm). Figure 2 shows the time-integrated SRS light from a hohlraum shot recorded on the FABS [2 (b)] and the NBI. The FABS has a shadow in the shape of a "Y" that is due to the mount holding the final laser turning mirror. There is a region between the FABS and NBI that is not measured and there are cutouts on the scatter plate where no measurement is made. Interpolation and extrapolation methods in the data analysis provide an approximate reconstruction of this missing data. The calibration system consists of both CW and pulsed light sources. The backscatter system includes redundancy in the measurements in order to apply standard self-checking techniques to verify error, to monitor when any instruments fail, and to provide

some level of backup if any instruments miss data. Table I lists the major requirements for the backscatter system.

TABLE I. Backscatter system requirements

Power accuracy	Time resolution	SBS spectral res.	SRS spectral res.
15% error at 15% scatter <sup>a</sup>	0.4 ns	0.06 nm	10 nm

<sup>a</sup> At 5% backscatter the allowed error is 25% and at 2% backscatter the allowed error is 50%.

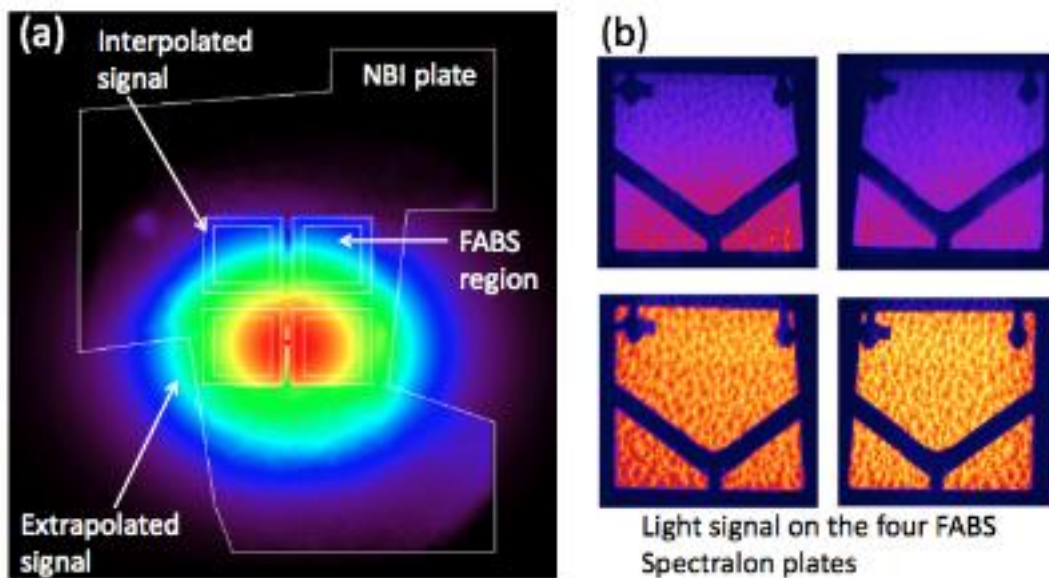


FIG. 2. SRS backscattered light from a cryo hohlraum target illuminates the lower-center region of the (a) NBI scatter plate and the (b) FABS. There is a clear downward shift visible in the scattered light distribution in both systems. The shadow from the "spider-mount" holding the final laser mirror is visible in the FABS images.

The organization of the remainder of this paper is as follows. Section II describes the FABS, Section III describes the NBI, Section IV describes the calibration system and error estimates. Section V gives a summary and conclusion.

## II. FABS

The FABS instrument, sketched in Fig. 3, measures the energy, power, and spectra of the backscattered light from the target which is collected by the incident light aperture. There are two FABS instruments on NIF and each one is designed to measure the backscatter on a 2-by-2 set of 4 beams called a "quad." One FABS is placed on an "inner" beam cone for a hohlraum target and the other is on an "outer" beam cone. The inner cone beams propagate further into the hohlraum before reaching the wall as compared to the outer beams. Infrared laser power (at 1053 nm) on its way to the target chamber reflects from the final laser turning mirror (LM8) before passing through the frequency conversion crystals, wedge focus lens (WFL), and other optics which focus it onto the target. The backscattered light propagates back down the beamline, transmits through the LM8 and enters the FABS instrument. The light then strikes a spectralon plate where it is diffused in a nearly Lambertian pattern. Eight optical fibers collect a small fraction of the light and deliver it to fast diodes, slow diodes, streaked spectrometers, and time-integrated spectrometers.

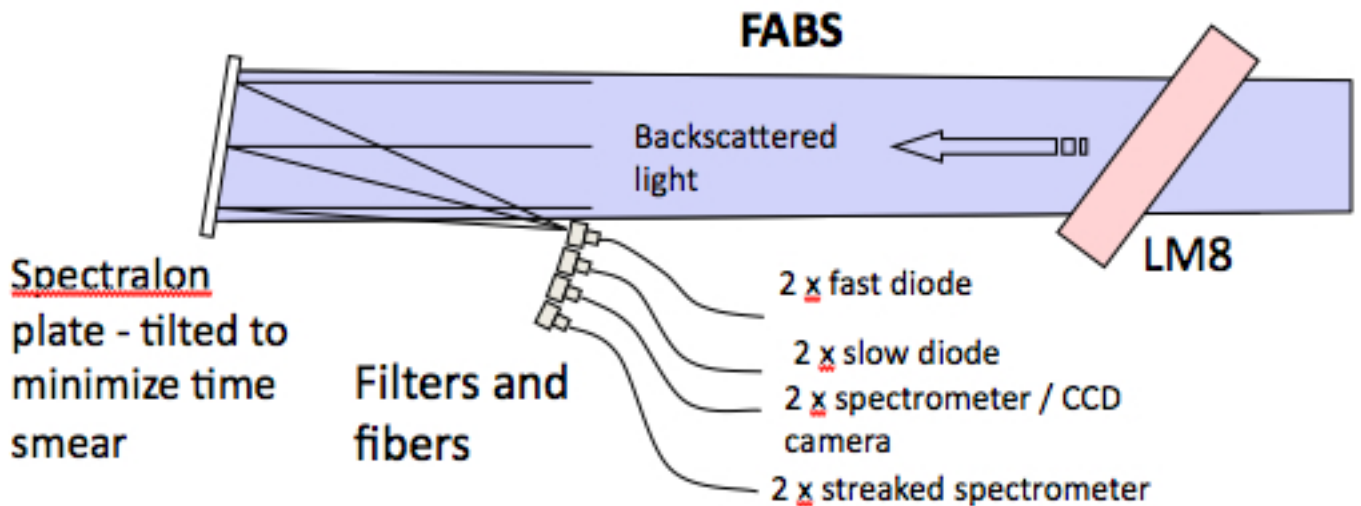


FIG. 3. Sketch of the FABS system showing light passing from the target through the final laser turning mirror and onto the spectralon diffuser plate. Eight fiber-fed instruments measure different aspects of the light.

One significant challenge to measuring backscattered light on large laser systems is that there is too much light. A significant fraction of it must be thrown away (leaving behind a  $10^{-10}$  fraction of the original light) before it reaches the detectors. This is accomplished in

FABS by directing the light to a spectralon (scatter plate) diffuser and collecting a fraction of the scattered light with a small fiber placed a long distance away. The Spectralon scatters the light in a nearly Lambertian pattern with a wavelength-independent efficiency. It has a measured damage threshold of about  $3 \text{ J/cm}^2$ [11] which corresponds to about 70% backscatter on a 1 megajoule shot. Eight  $200\text{-}\mu\text{m}$  radius fibers are placed 2.5 m from the Spectralon to collect a fraction of the scattered light given as  $(r/R)^2 = (0.02/250)^2 = 6.4 \times 10^{-9}$ . This light is transported through the fiber to one of a number of detectors. Figure 4 shows the Spectralon plates and the fiber pickoffs for one of the FABS systems.

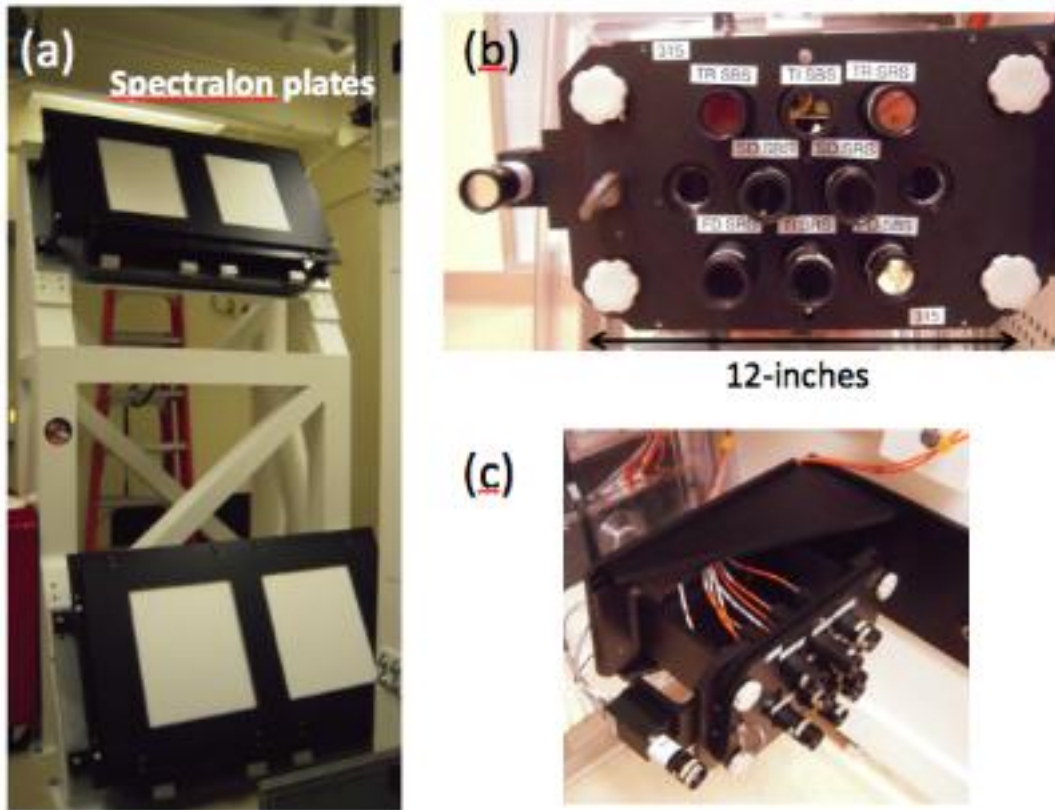


FIG. 4. (a) The four spectralon plates with black masks are the diffusers for light backscattered into the final optics aperture. The plates are about 43 cm x 50 cm. (b) A removable plate holds filters in front of each fiber to attenuate the signal level and fix the spectral band of light entering the fiber. (c) Another view of the filter plate shows the fibers that transport light to the various detectors.

Four of the fiber pickoffs measure SBS signals (350 - 353 nm) and the other four measure SRS signals (450 - 750 nm). The instruments are selected for operation in these spectral

bands. Filters placed in front of the fibers select the wavelength band of interest, tailor the wavelength transmission to make some of the detectors "color-blind", and attenuate the light coupled to the fibers.

ST400E Mitsubishi step-index fiber is used exclusively for the FABS system. This is 400  $\mu\text{m}$  core diameter fused silica fiber that has better transmission in the UV than the graded index version of the same fiber. The mode and chromatic dispersion[13] for the lengths used allow meeting the required  $\leq 0.4$  ns temporal resolution.

## II (a). Fast photodiodes

Hamamatsu R1328U-53MOD fast phototubes with an extended S-20 photocathode measure the calibrated power time-history of the backscattered light for both SRS and SBS. These diodes have an intrinsic response time of 60 to 80 ps. Output signal from the diode is coupled to a high-bandwidth (LMR600) coax cable of about 40 ft length which carries the signal to a fast Tektronix DPO70404 scope. We have characterized the dispersion in the long cable and can correct for this. However, in practice we find that it is not necessary to make this correction.

Precision calibration of the fast diode is done using a pulsed laser from TCC. We will describe this later. A separate check of the diode coupling to the spectralon plate (without the effect of the beam line) is done using a minilite pulsed laser (Coherent). The laser produces an out put power of about 17 mJ at 532 nm and is used locally near the spectralon. This measurement gives a diode sensitivity which ranges from about  $2.3 \times 10^{-9}$  V/W to  $5.1 \times 10^{-9}$  V/W over the four beams. An estimate of the sensitivity gives a value which is comparable to what is measured. Thus, fiber coupling is  $6.4 \times 10^{-9}$  (see above); diode sensitivity at 532 nm is measured as 0.028 A/W; diode output is a  $50\Omega$  source in parallel with a  $50\Omega$  load; attenuation of the LMR600 cable is about a factor of 1.5. Combining these gives:  $6.4 \times 10^{-9} \times 0.028 \times 25/1.5 = 3 \times 10^{-9}$  V/W. This measurement provides a useful check that the system is working as expected; the transmission through the beam line can be applied to this sensitivity to obtain the approximate diode calibration relative to TCC.

## II (b). Slow photodiodes

The slow diodes provide a calibrated measure of the energy (redundant with integrating the fast diode) although they can also provide a slow time-response power measurement. The diodes are Electro-Optic Technology Inc.[15] ET-2020 biased detectors with a time response of about 2.5 - 3 ns. The signal from two diodes is multiplexed onto a single channel of a Tektronix DPO7104 scope with a 100 ns time separation. This timing difference is achieved with an additional 20 m of fiber.

Precision calibration of these diodes is also done using a pulsed laser at TCC. However, as with the fast diodes coupling to the spectralon is measured at 532 nm using the minilite laser. This gives a sensitivity ranging from  $7 \times 10^{-9}$  V/W to  $7 \times 10^{-8}$  V/W over the four beams. Estimating the sensitivity, as for the fast diode, the output couples to a  $50 \Omega$  load and the sensitivity is 0.3 A/W at 532 nm. This gives:  $6.4 \times 10^{-9} \times 0.3 \times 50/2 = 4.8 \times 10^{-8}$  V/W.

## II (c). Optical filters

The SRS and SBS wavelength bands are selected with bandpass filters. The SBS filter transmits about 60% at 351 nm and has a width of about 50 nm. The SRS filter transmits about 98% of the light in the range of 450 nm to 750 nm.

Both the fast and slow photodiodes have wavelength-dependent response characteristics; the detectors typically respond more strongly to longer or shorter wavelength light. Broad-band (SRS) measurements using the diodes "as-is" require post-shot analysis that corrects the measured signal for the detector color sensitivity based on knowledge of the SRS time-dependent spectral content. This information can be obtained from a spectral streak, for example. If the diode is corrected in this manner than it cannot possibly provide an independent power measurement as its interpretation relies on the spectral streak which becomes the primary power measurement. At best, it can only provide a consistency check on the spectral streak data. One of the design goals for the FABS was to make the fast and slow diode instruments independent. The way this was done was to design a "flattening" - filter. This filter alters the color sensitivity of the diode making it "color blind" to light from TCC. This removes the need to perform post-shot analysis relying on the spectral streaks. The resulting fast diode trace can be converted to the backscattered SRS power (in that partic-

ular beam) by multiplying by a constant. Likewise, the slow diode signal integral can be converted to energy (in that beam) by multiplying by a constant. Advanced Thin Films[14] designed and built these flattening filters for the fast and slow SRS diodes in FABS and the SRS cameras for NBI.

Metallic ND filters attenuate light reaching the fibers. The advantage of metallic filters is that they can have a nearly wavelength independent transmission from 450 nm to 750 nm. The disadvantage of metallic filters is that two or more create an etalon when mounted parallel to each other. This increases the light transmitted through the filters. The slight time-delay of the reflected signals is within the time-resolution of the instrument so it is not detected. This etaloning effect is mitigated on the NBI instrument by tilting the filters at alternating + and - 10-degrees relative to the normal filter orientation. Tilting the filters increases the thickness of the metallic coating that the light passes through. This was easy to take into account. The filters were not tilted on the FABS instrument so the enhanced light transmission had to be accounted for in the data analysis. Offline characterization of the different metallic filter arrangements used in the experiment provided a measurement of the enhancement factors. Calculations of light transmission through glass with conductive metallic coatings showed approximate agreement with the measurements. The preferred method of operation is to use tilted metallic filters in order to simplify the post shot analysis.

#### **II (d). Time-integrated calibration spectrometer**

The primary calibrated energy measurement is made with the calibration spectrometer. Eight fibers transport SRS and SBS light from each of the 4 beams of one FABS to the slit location of a McPherson 2035 spectrometer. This is an 0.35 m focal length spectrometer with a 100 l/mm grating giving a measured dispersion at the output of 29.4 nm/mm. The 400  $\mu\text{m}$  diameter fibers are apertured with a 200  $\mu\text{m}$  slit and are stacked vertically at the input. The output of the spectrometer is imaged onto a PI-Max gated ICCD camera (model 7361-0001) which provides a 512 by 512 pixel image having wavelength in the horizontal direction and fiber-number in the vertical direction. The light is dispersed in first order for the SRS band and in second order for the SBS band. The camera is gated at 30 to 50 ns in order to gate out light that is not part of the main backscatter signal and may come from other reflections at earlier or later times. This instrument is absolutely calibrated using a

Xe lamp at target chamber center (TCC).

## II (e). Time-resolved spectral measurements

The SRS and SBS time-resolved spectra are measured with a spectrometer combined with a streak camera. Each spectrometer multiplexes the signal from four fibers, one from each beamline, in a way described by[13]. Two of the four fibers are delayed 15 ns relative to the others in order to displace them in time on the streak. A typical streak record is shown in Fig. 5. The SRS measurements utilize an Acton SP2150i spectrometer (1/5-meter) with a 150 l/mm grating giving a measured dispersion at the spectrometer output of 42.2 nm/mm. The input fiber arrangement is imaged with approximately a magnification of 1.1 onto the streak camera. A GSCP streak camera with an S-20 photocathode coupled to a CCD camera creates the streak record. The active part of the entrance slit is about 20 mm wide and the streak speed is set to 40 ns over the entire record. The CCD image is a 1365 x 1365 pixel image. Chromatic dispersion in the fiber leads to a wavelength-dependent variation in the arrival time for the different wavelengths in the SRS signal; red arrives before blue. Measurements of this delay show it to be in agreement with calculations using the Sellmeier coefficients for fused silica fiber[13]. The delay is easily removed during analysis of the data.

Time-resolved spectral streaks of the SBS light are measured and multiplexed the same way as the SRS streaks. The SBS spectrometer is a McPherson 207 1-m spectrometer with a 2400 l/mm grating in second order for the 30° FABS and a McPherson 2061 3/4-meter spectrometer with a 2400 l/mm grating in second order for the 50° FABS. The measured dispersion for the 207 is 0.51 nm/mm and 0.37 nm/mm for the 2061. The streak camera is set at 40 ns for the entire record.

Figure 6 shows the SRS and SBS from gaspipe experiments. In these experiments the target is a 7 mm long, 2 mm diameter CH tube filled with either C<sub>5</sub>H<sub>12</sub> (for SRS) or CO<sub>2</sub> gas (for SBS) at 1 atm. The ends of the tube are covered with 2 μm thick polyimide and the axis of the tube is aligned along the direction to the single beam quad being used as the pump. The purpose of these experiments was to generate strong SRS and SBS for verifying the operation of the backscatter instruments. Figure 6 (a) was obtained using the backscatter system on Q31B and (b) used the system on Q36B. The SRS shows a rapidly

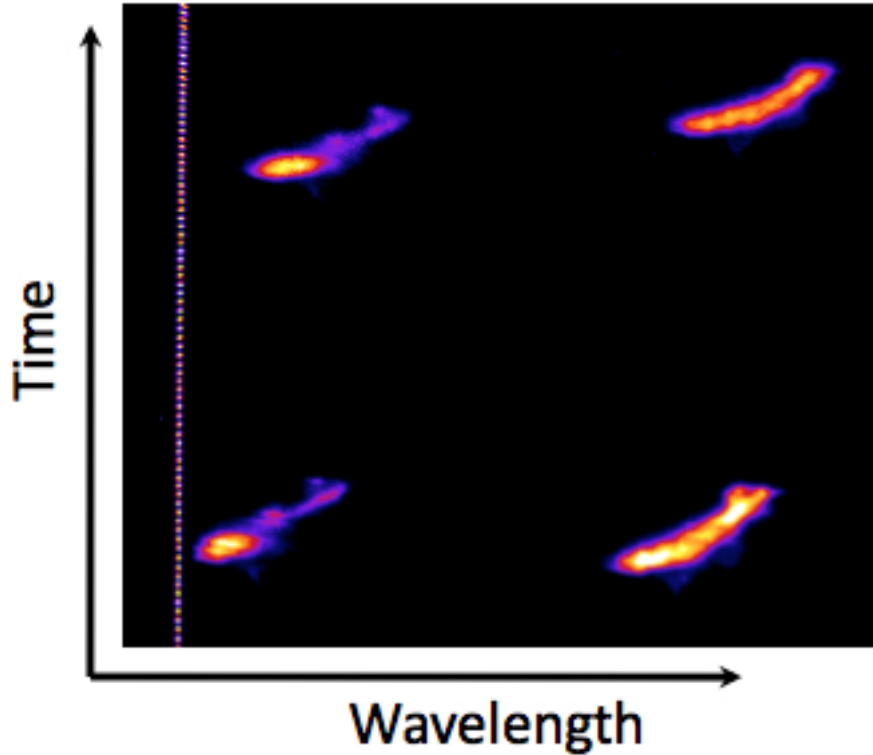


FIG. 5. Image shows the SRS spectra from the four beams on the  $30^\circ$  quad for a 1 MJ energy shot into a cryo hohlraum. All four spectra shows an increasing shift to the red with increasing time. Evidence of the amplitude modulation from the laser bandwidth (smoothing by spectral dispersion) is visible in the lower left spectra. Also visible in the image on the left is the series of pulses from the comb generator.

downshifting spectral signal during the incident laser pulse. Backscatter simulations show almost perfect agreement with this spectral measurement and indicate that the scattering is coming from a region of rapidly decreasing density due to laser heating of the plasma. The starting wavelength (560 nm) of the SRS light corresponds to the  $\sim 11\%$  critical density seen by the laser during the initial ionization of the 1atm of fill gas. The SRS signal starts with a red shift of about  $8 \text{ \AA}$  and shows a decrease to about  $6.5 \text{ \AA}$ . This indicates that the location of the scattering is moving into slightly cooler plasma.

Figure 7 shows the SRS spectra summed over the 4 beams in the quad for two hohlraum shots. The lower energy shot, (a), has a lower pressure of hohlraum gas fill (210 Torr) than the higher energy shot, (b), which has 330 Torr. In both cases the SRS shows an increasing wavelength shift during the peak power of the laser. The backscatter level is higher in (a)

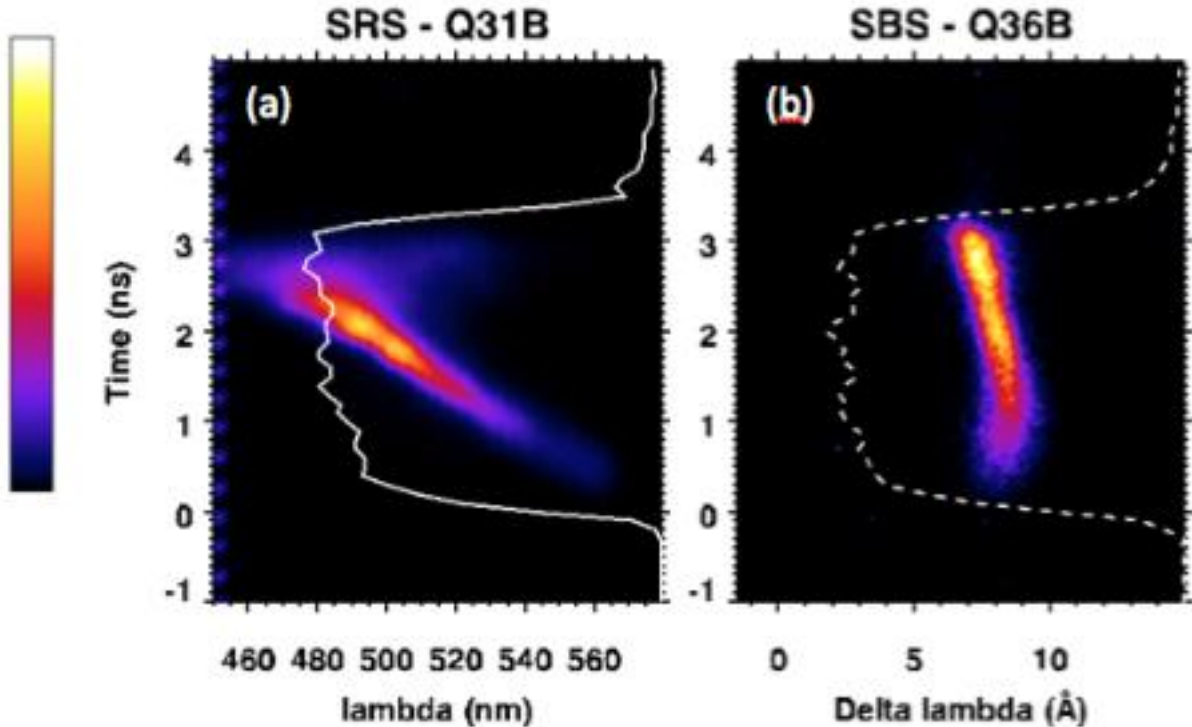


FIG. 6. (a) shows the backscattered SRS spectrum summed over the 4 beams for a gaspipe experiment with  $C_5H_{12}$  fill at 1 atm. (b) shows the backscattered SBS spectrum summed over the 4 beams for a 1 atm filled  $CO_2$  gaspipe.

than in (b) and the Raman extends to a slightly higher wavelength at the end of the pulse in (b) than in (a). This may be due to the overall lower backscatter in (b). Current efforts are focused on developing consistency between the hohlraum hydrodynamic simulations and the resulting post-processed backscatter SRS and the measurements.

### III. NBI

The Near Backscatter Imager (NBI) system consists of a scatter plate mounted inside the target chamber and centered on a quad of beams and two viewing cameras, one for SRS and one for SBS. There are two of these systems; one for each quad used for backscatter measurements. The purpose of the NBI is to measure light backscattered outside of the incident optics aperture. A slow diode with scatter plate visibility is placed next to each camera to provide timing information for the cameras. We have built for the first time a time-resolved NBI detector which utilizes a distribution of 40 fibers and a streak camera

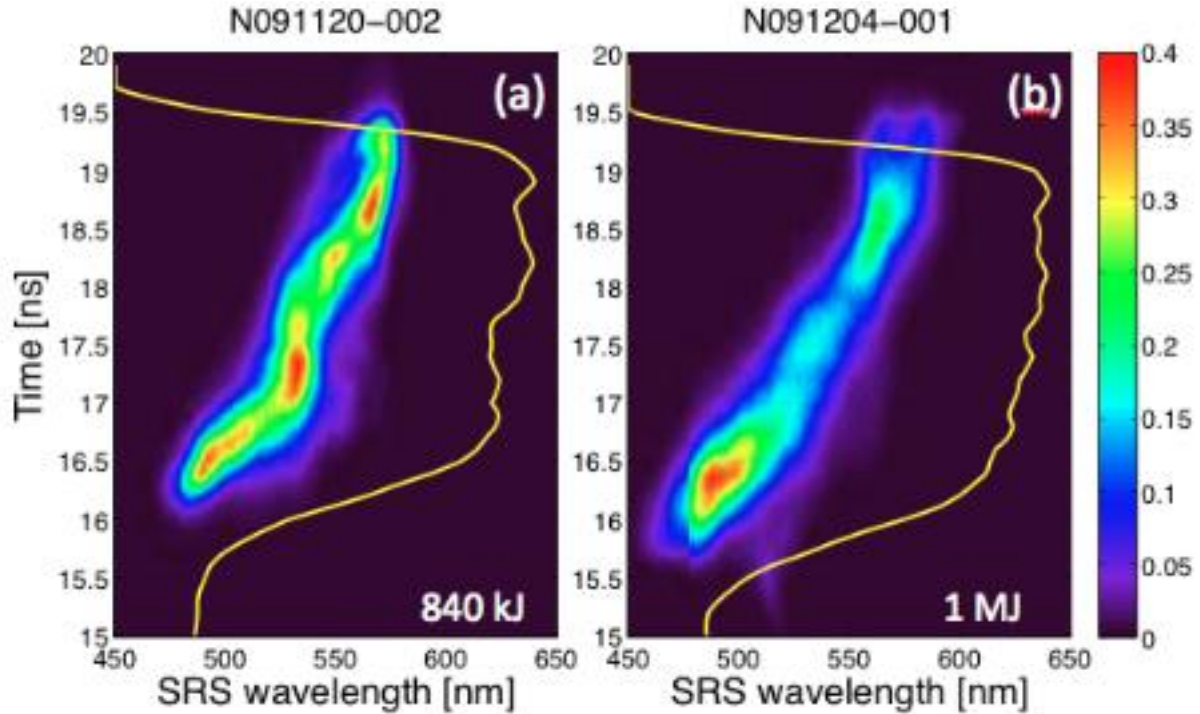


FIG. 7. The backscattered SRS spectrum summed over the 4 beams of the quad is shown for hohlraums where (a) the gas fill is 210 Torr of He and (b) the gas fill is 330 Torr of He.

to measure the time-history of the backscattered light spatial distribution on the scatter plate. This instrument can be configured to look at either SRS or SBS. Figure 8 shows the configuration of the NBI system in the target chamber.

## NBI sketch goes here

FIG. 8. This shows a sketch of the key components of the NBI system.

### III (a). Scatter plate

Figure 9 shows the two scatter plates as seen in the NIF target chamber; both plates share the same design. The plates measure 1.5 m x 1.8 m and consist of protective borofloat glass on top of 7 mm thick spectralon which sits on a surface of aluminum held in place by a steel frame positioned with kinematic mounts. The plates have several cut-outs to avoid

unconverted laser light from beams on the opposite side of the target chamber. A  $2\mu\text{m}$   $\text{B}_4\text{C}$  coated boundary and clips hold the glass and spectralon on the Al surface. The  $\text{B}_4\text{C}$  coating distributes the absorption of x-rays from the targets over a larger volume and reduces the possibility of metal ablation onto the scatter plate glass. The primary purpose of the glass coating is to protect the spectralon from x-ray flux generated by target shots. In addition, target debris deposits on the glass which can be replaced more easily than the spectralon.

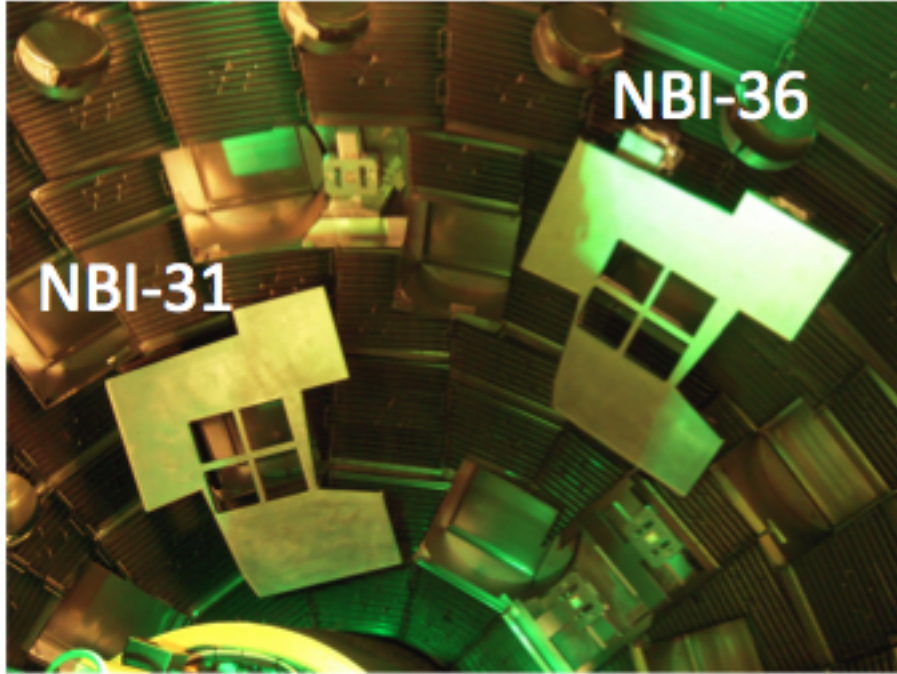


FIG. 9. Image shows the two NBI scatter plates positioned in the NIF target chamber.

### III (b). NBI camera detectors and filters

The ICCD cameras are PI-Max (model 7467-0022) with a  $1024 \times 1024$  pixel array. The large number of pixels is required to meet the spatial resolution specification. Obtaining a measure of the light distribution along the thin "cross" section of the plate that lies in between the four beams is important for estimating the signal in the unmeasured region between the beam aperture (measured by FABS) and the NBI plate. A single camera pixel corresponds to about a  $2.4 \text{ mm}$  square region on the plate. Thus, there are at least 16 pixels within the thin part of the "cross" which is a sufficient number for estimating the intensity dependence without edge effects. The camera is gated for  $50 \text{ ns}$  in order to accommodate a

range of pulse shapes from several ns to 20 ns used in laser experiments. Camera sensitivity varies some during the gate; the gate is timed so that the majority of backscatter signal arrives in a region of the gate with fairly constant sensitivity. Signal from different parts of the plate arrive at different times due to the large spatial extent of the plate. The spread in this arrival time is about 5 ns and easily falls within the gate time of the camera. The f/stop for both cameras is set to f/16 and the image size is adjusted to fill as much of the CCD as possible.

The NBI system filters are similar to the ones used for the FABS system except they are 2-inches in diameter. Bandpass filters select the SRS or SBS band. A special flattening filter makes the SRS camera colorblind and metallic ND filters attenuate the signal. A special holder was designed for the ND filters to tilt them and mitigate etalon effects.

### **III (c). Time-resolved NBI detector**

A time-resolved NBI instrument measures the time-history of the backscattered light distribution on the scatter plate. An optical system images the scatter plate, demagnified 17 times, onto a flat plate. The plate contains forty 400- $\mu\text{m}$  diameter optical fibers placed at strategic locations for sampling light on the plate. This fiber size collects significant light while still allowing alignment of the fiber pattern to the cross part of the scatter plate without encountering edges. These fibers then connect to a fiber taper reducing the diameter to 200- $\mu\text{m}$ . The tapers connect to 2-m of 200 $\mu\text{m}$  fiber which terminate in a linear array and couple to the input slit of a streak camera. Several more fibers are added to the array to provide comb and fidu signals. Figure 10 (a) shows the scatter plate location seen by each fiber and 10 (b) a sample of the streak data. Filters select either the SRS or SBS band, flatten the photocathode response of the streak camera, and attenuate the signal before it enters the fibers.

Light reaching the camera is streaked in time to give the temporal evolution of the light intensity at the 40 fiber locations on the plate. Analysis of the data involves setting the absolute time of the streaks and the absolute amplitude. The different arrival times of the light from various parts of the plate is corrected using the geometrical distances from the target to the plate. We verified this timing correction for the fibers using amplitude modulations in the NBI light which are produced from AM in the incident beams due to

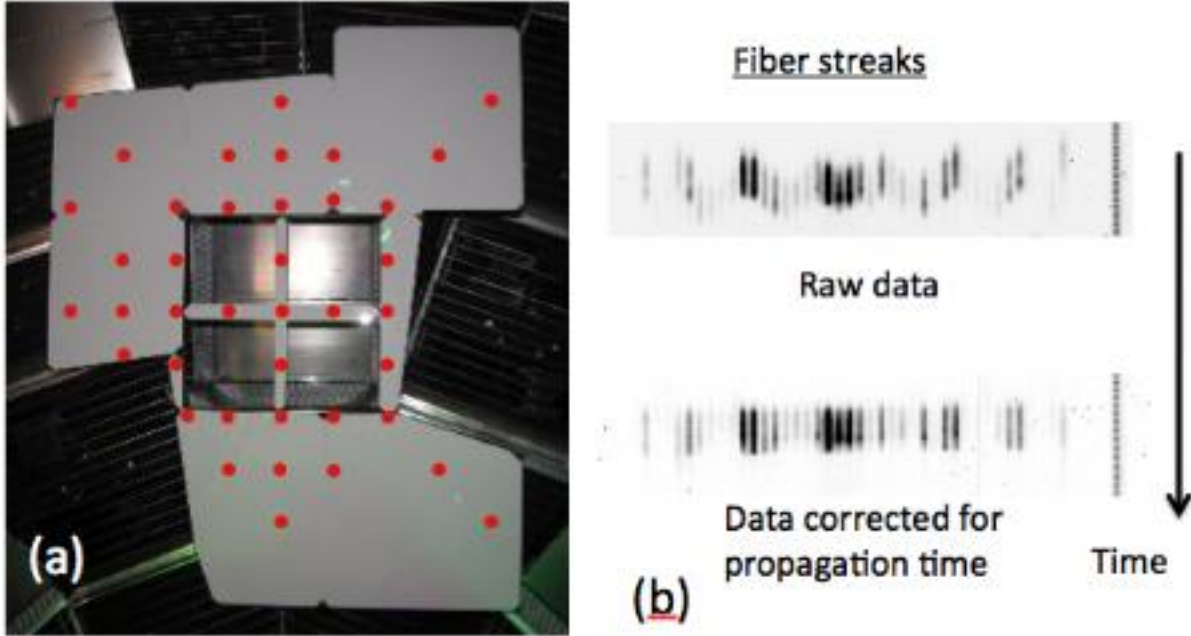


FIG. 10. (a) Image shows the approximate location of the view for each of the 40 fibers collecting signal from the scatter plate. (b) The top image shows the resulting streaks (with comb signal) for a target shot. During analysis, the arrival time for the fibers is corrected leading to the lower image with the fiber arrival times adjusted to be the same for all fibers..

SSD. The absolute amplitude of the streaked time-histories is normalizing to the the time-integrated signal measured at the plate location corresponding to the fiber. The streaks become a plot of  $W\text{cm}^2$  as a function of time at the fiber location on the scatter plate. Bi-linear interpolation fills in the regions of the plate between the 40 points and creates a snapshot of the backscattered spatial intensity distribution on the plate every 100 ps. These snapshot images are assembled into a movie which shows the temporally evolving backscattered light intensity on the NBI plate.

Many of the cryo hohlraum experiments show a deflection of the SRS downward toward the hohlraum axis. As the laser pulse-shape enters the high intensity region near the end of the pulse the SRS NBI pattern shows movement downward and then back up as the laser turns off. Figure ?? shows the time evolution of the NBI spatial distribution during the high-intensity part of the pulse. Comparisons with modeling are ongoing and will help verify that the hohlraum hydrodynamics and refraction of the SRS light are computed consistently with the experiment.

Another important result obtained from this measurement is that the temporal evolution of the total backscatter (FABS + NBI) is nearly identical to the time-history of the FABS signal.

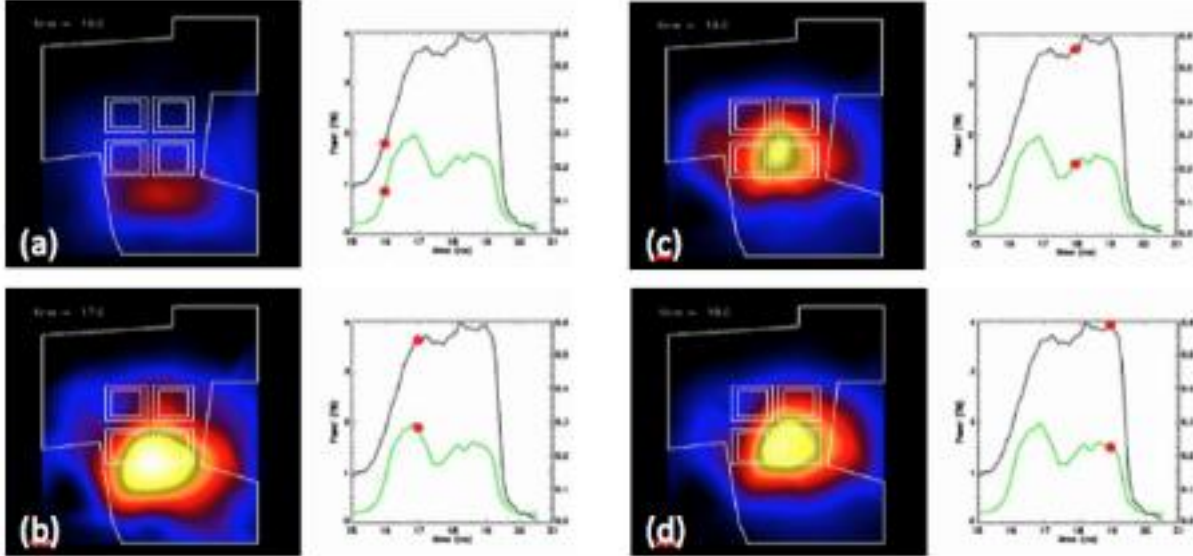


FIG. 11. Image shows the evolution of the spatial pattern on the NBI scatter plate for SRS. Stepping through the images in order the times are 16 ns, 17 ns, 18 ns, and 19 ns.

### III (d). NBI plate vulnerabilities

The glass covering the spectralon is vulnerable to transient x-ray darkening and debris buildup. X-rays can generate transient free electrons in the glass making it act as a semiconductor and increasing the absorption of optical light. This process was investigated experimentally on the Omega laser[6] by Froula[16] in 2007 and London developed a physics model for the x-ray induced transient darkening of borofloat glass based on the measurements. Extrapolating the model to NIF we have estimated that the effect may lead to an underestimate of the backscatter by as much as 10% to 40%. The observed similar pulse shapes of the FABS time-history and the NBI time-history suggest that the effect is small (in the 10% range). There remain a number of significant uncertainties in the model which would be resolved with additional experiments at longer wavelengths

Debris build[17] has been observed on the NIF NBI plates. Figure 12 shows the NIF scatter plates when first installed and after more than 50 shots (most of them hohlraum

targets). There is ongoing work to determine what the debris is and the rate of buildup but it appears to be a thin metallic film with material from the targets and the first wall. The backscatter light is intense enough to remove the debris from the scatter plate glass in certain regions. This is what creates the significant contrast between light and dark regions on the plate. The calibration laser was discovered to have sufficient intensity to partly or completely remove debris from the glass and therefore became of non-perturbative calibration method in the regions with debris. Our present view, based on observations, is that laser shots create a source of debris that coats the scatter plate approximately uniformly but the backscatter light is intense enough to remove most or all of the debris on the plate region where the scattering must be measured accurately.

#### **IV. CALIBRATION**

Requirements on the backscatter measurements (see Table I) consist mainly of power accuracy, temporal resolution, and spectral resolution. Several techniques are utilized to show that the instruments meet these requirements. Achieving these requirements is important for reaching an accurate understanding of the hohlraum energetics and providing specific experimental signatures that guide simulations of the hohlraum hydrodynamics.

##### **IV (a). Spectral calibration**

Mercury and Neon calibration lamps[18] provide lines which are used to calibrate the dispersion and offset wavelength of the SRS and SBS spectrometers. Some target shots produce scattered 351 nm and unconverted 527 nm light which is visible on the spectrometers and provides a way to periodically verify the wavelength offset.

##### **IV (b). Temporal calibration**

The streaked spectral instruments and the fast diodes require identification of  $t = 0$  relative to the laser pulse and the streaked instruments require calibration of the sweep rate. Timing shots establish the  $t = 0$  of the SBS instruments. These shots consist of firing a short 0.09 ns UV laser pulse onto a flat gold disk. The backscattered light signal creates a

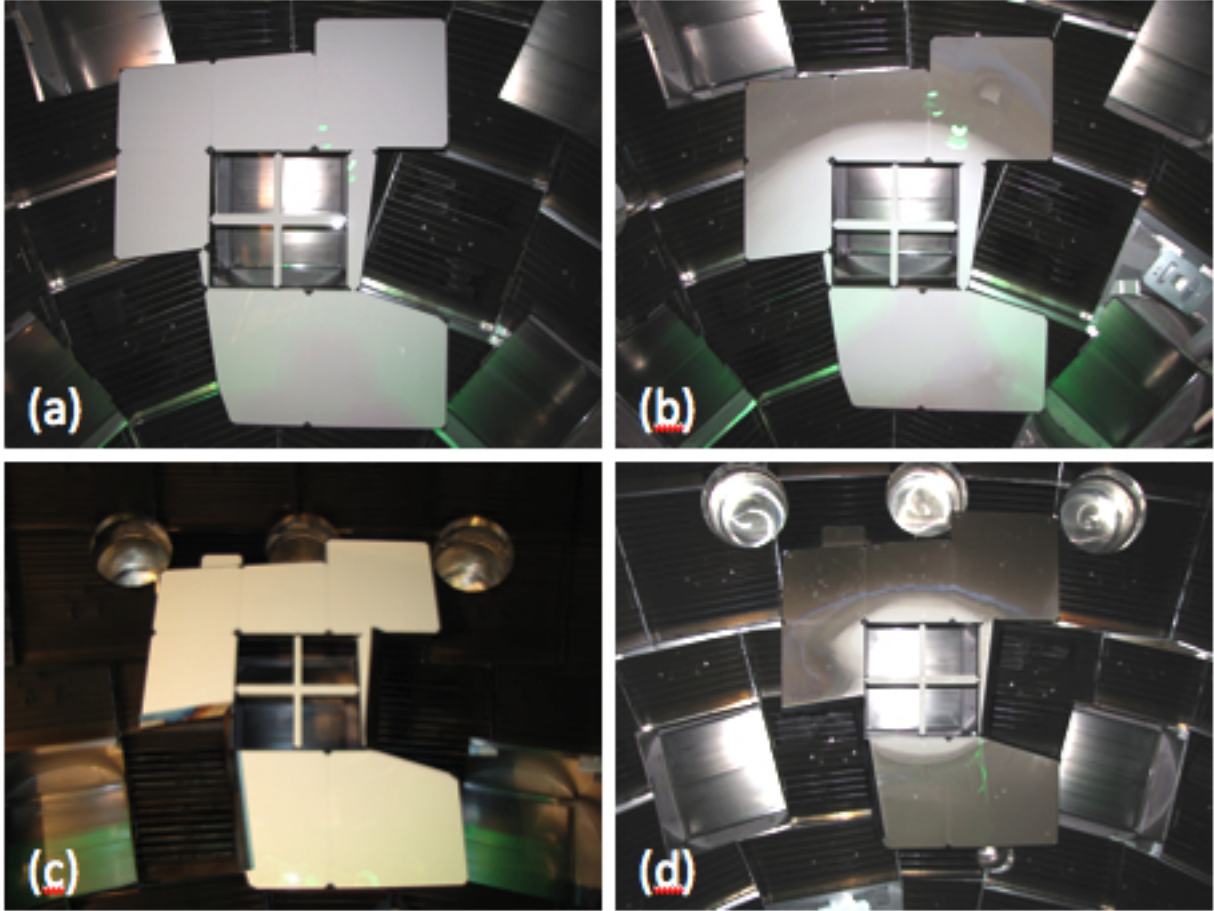


FIG. 12. (a) NBI scatter plate at  $30^\circ$  with fresh glass. (b)  $30^\circ$  NBI plate with debris band visible in the upper portion of the scatter plate. (c) Scatter plate at  $50^\circ$  with fresh glass. (d) Debris on the scatter plate shows a tight region around the quad where there is little to no debris. Also visible in (b) and (d) are small spots where the calibration laser removed plate debris.

short burst on the fast diodes and the SBS streak cameras indicating the location of  $t = 0$ . Timing shots provide little or no SRS light so a different method is used. Shots useful for setting the SRS  $t = 0$  are shots with 1) SRS lasting the entire laser pulse, 2) SRS continuing to the end of the laser pulse and 3) a flash of SRS at the start of the laser pulse. Utilizing several shots like these allows identifying the  $t = 0$  on the SRS streaks and fast diodes to within about 0.15 ns. In addition to setting the  $t = 0$ , the streak cameras have an in-situ measure of their sweep speed. This can vary by up to 5% over the sweep record. Each camera utilizes a comb generator which produces a train of pulses at either 3 GHz or 6 GHz at about 810 nm. This comb signal is projected directly onto the streak camera slit (near

the edge) and provides a monitor of the sweep speed at one horizontal slit location for each streak camera image. This is sufficient to meet the temporal resolution requirements for the spectral streaks.

#### **IV (c). Energy calibration**

The calibration spectrometer provides the primary energy measurements. This instrument is calibrated with a 300 W Oriel/Newport calibrated Xe lamp placed in the center of the target chamber. Light from the lamp is directed off of a mirror so that it can be pointed easily. The virtual image of the light filament is positioned within several mm from TCC. Light from the lamp illuminates all 4 beamlines of one quad at a time. Light also falls on part of the NBI plate and allows a secondary calibration for the scatter plate (discussed below). Lamp light reaching the spectralon in FABS is collected by two fibers per beam and transported to the calibration spectrometer. Only the bandpass filters are kept in front of the fibers for this measurement.

The calibrated emission of the lamp and the FABS geometry allows a determination of the calibrated energy per nm per pixel count. The calibration typically requires 10 minutes for good signal. The "spider mount" that holds the final turning mirror [visible in Fig. 2 (b)] creates a shadow that blocks 20% of the beam area. We assume that this region is filled in with light at similar intensity to the neighboring regions. Calibration is done with the camera in shutter mode so that it can collect light for many seconds. During a shot the camera is run in gate mode so that secondary reflections can be gated out of the total camera signal. Measurements show that the camera is 1.5 times more sensitive when in shutter as compared to gated mode. This factor is accounted for in the calibration.

#### **IV (d). Power calibration**

Two different pulsed lasers from Coherent are used for power calibration of the fast diodes (one was discussed earlier in Section II (a)). These lasers are also used for energy calibration of the slow diode, to verify the calibration spectrometer, and to verify the wavelength offset for the SRS streak camera. One is the minilite laser (17 mJ at 532 nm) and the other is a Surelite laser capable of about 200 mJ of 532 nm and about 100 mJ of 355 nm laser light in

a 4 ns Gaussian.

The Surelite laser is directed to TCC from outside the target chamber. It then reflects from two mirrors (one of them is remotely pointed) and is directed into one of the FABS beams and onto the FABS spectralon. Calibrating the FABS instruments this way includes the effects of the beam optics which have wavelength and polarization-dependent transmission. In order to account for polarization a quarter-wave plate is used to rotate the laser polarization in increments of  $10^\circ$  while measuring the energy on the calibration spectrometer. The calibration used for experimental analysis is the average of the max and min over the range of polarizations. The higher energy in the surelite allows calibration of the fast and slow diodes with the flattening filters in place. Different locations on the spectralon show up to a 10% measurement variation and different sized laser spots ranging from about 2 cm to 10-inches show less than 5% measurement variation.

The surelite laser is also used for NBI calibration. There are two configurations for this calibration; one utilizes TCC and one doesn't. These two options provide greater flexibility for scheduling calibration time with other target area activities. An adjustable mirror located at the chamber access port directs the laser beam either to TCC or directly to the scatter plates to a predefined number of locations where the sensitivity is measured. The number of points is determined by the time available for calibration. Each point requires about 30 to 45 sec. A standard calibration consists of measuring sensitivities on both scatter plates at both 532 nm and 355 nm. Keeping the calibration activity to 2 hours or less allows about 45 points per scan. Currently, 30 points are used and the plan is to increase this in future scans. Translating the data points to a calibration map is performed the same way as is described in [17]. The TCC NBI calibration configuration is identical to the FABS calibration but the laser is directed onto a series of points on the scatter plate rather than down into FABS.

#### **IV (e). Error estimates**

Off-line measurements of temporal and spectral resolution show that the instruments meet or exceed the requirements for these parameters. The power measurement uncertainty arises from variations in or approximations to the instruments, optics, and geometry of the system. In some cases, the behavior of an instrument is complex but it is approximated in simple terms with an uncertainty specification. The overall uncertainty does not include

unknown systematic errors.

The FABS and NBI systems contribute differently to the error in the total power measurement. The largest error in FABS comes from approximating the transmission through the final laser turning mirror (LM8). Near 351 nm the transmission through the mirror is decreasing rapidly with decreasing wavelength. In addition, the transmission is significantly different between S and P-polarized light. The calibration of UV transmission through this mirror is chosen to be the average transmission from 350 nm to 353 nm and the average of the S and P-polarizations. This gives a single transmission value with an uncertainty of  $\pm 18\%$ . A similar approach is taken for the SRS; however, the variation in transmission with polarization and wavelength is smaller than in the UV. Choosing a transmission which is the average over the polarization and the wavelength oscillations gives a resulting SRS uncertainty of  $\pm 14\%$ . Added to this transmission uncertainty is 8% error in the calibration of the fast diode and 4% error in the filter calibration. These uncertainties are not correlated so adding them in quadrature gives a more representative outcome than adding them up directly. The overall error is  $\pm 17\%$  for SRS and  $\pm 20\%$  for SBS.

The NBI system has uncertainties that arise from calibration, temporal evolution, and analysis that interpolates and extrapolates to regions with no plate material. The calibration uncertainties are estimated to be  $\pm 8\%$  and the analysis uncertainties are approximately  $\pm 8\%$  based on studies using different analysis techniques. The temporal evolution of the full backscatter is observed to be well represented with the FABS temporal evolution with an error approximated as  $\pm 5\%$ . Additional uncertainty from filters is estimated to be  $\pm 4\%$ . Combining these as uncorrelated errors gives  $\pm 13\%$ .

The NBI typically represents 2/3 of the backscatter signal and the FABS is 1/3. If there are 3 units of backscatter then 1 unit is in FABS and 2 on NBI. The uncertainty in FABS is 0.2 units and on NBI it is 0.26 units. We estimate the total uncertainty as the sum of these to obtain a worst case. This gives a total uncertainty of 0.46 units or  $\pm 15\%$  which meets the requirement. Different fractions of light into FABS and NBI as well as degradation in optics from debris or damage increases this error.

## V. SUMMARY

Backscatter measurements on NIF utilize a FABS and an NBI instrument on two different quads. A suite of techniques is used to calibrate energy and power measurements and set the timing offset, sweep speed, and wavelength offset of other instruments. The power uncertainty is estimated to be  $\pm 15\%$  at best. A new time-resolved NBI instrument shows that the overall time-history of the backscatter is very similar to the pulse shape obtained from the fast diode signals.

This work was performed under the auspices of the U. S. Department of Energy by the Lawrence Livermore National Laboratory under Contract No. W-7405-Eng-48.

---

\* moody4@llnl.gov

- [1] Glenzer, S. H. and MacGowan, B. J. and Michel, P. and Meezan, N. B. and Suter, L. J. and Dixit, S. N. and Kline, J. L. and Kyrala, G. A. and Bradley, D. K. and Callahan, D. A. and Dewald, E. L. and Divol, L. and Dzenitis, E. and Edwards, M. J. and Hamza, A. V. and Haynam, C. A. and Hinkel, D. E. and Kalantar, D. H. and Kilkenny, J. D. and Landen, O. L. and Lindl, J. D. and LePape, S. and Moody, J. D. and Nikroo, A. and Parham, T. and Schneider, M. B. and Town, R. P. J. and Wegner, P. and Widmann, K. and Whitman, P. and Young, B. K. F. and Van Wonterghem, B. and Atherton, L. J. and Moses, E. I., *Science*, **327**, 1228, 2010.
- [2] E. I. Moses and C. I. Wuest, *Fusion Science and Technology* **47**, 314 (2005).
- [3] J. D. Lindl, *Phys. Plasmas* **2**, 3933 (1995).
- [4] Steven W. Haan, Stephen M. Pollaine, John D. Lindl, Laurance J. Suter, Richard L. Berger, Linda V. Powers, W. Edward Alley, Peter A. Amendt, John A. Futterman, W. Kirk Levedahl, Mordecai D. Rosen, Dana P. Rowley, Richard A. Sacks, Aleksei I. Shestakov, George L. Strobel, Max Tabak, Stephen V. Weber, and George B. Zimmerman, *Phys. Plasmas* **2**, 2480 (1995).
- [5] R. K. Kirkwood, C. A. Back, M. A. Blain, D. E. Desenne, A. G. Dulieu, S. H. Glenzer, B. J. MacGowan, D. S. Montgomery, and J. D. Moody, *Rev. Sci. Instrum.*, **68**, 636 (1997).
- [6] J. M. Soures, R. L. McCrory, C. P. Verdon, A. Babushkin, R. E. Bahr, T. R. Boehly, R. Boni, D. K. Bradley, D. L. Brown, R. S. Craxton et al., *Phys. Plasmas* **3**, 2108 (1996).
- [7] P. Neumayer, C. Sorce, D. H. Froula, L. Divol, V. Rekow, K. Loughman, R. Knight, S. H. Glenzer, R. Bahr, and W. Seka, *Rev. Sci. Instrum.*, **79**, 10F548 (2008).
- [8] D. H. Froula, D. Bower, M. Chrisp, S. Grace, J. H. Kamperschroer, T. M. Kelleher, R. K. Kirkwood, B. MacGowan, T. McCarville, N. Sewall, F. Y. Shimamoto, S. J. Shiromizu, B. Young, and S. H. Glenzer, *Rev. Sci. Instrum.*, **75**, 4168 (2004).
- [9] D. E. Bower, T. J. McCarville, S. S. Alvarez, L. E. Ault, M. D. Brown, M. P. Chrisp, C. M. Damian, W. J. DeHope, D. H. Froula, S. H. Glenzer, S. E. Grace, K. Gu, F. R. Holdener, C. K. Huffer, J. H. Kamperschroer, T. M. Kelleher, J. R. Kimbrough, R. Kirkwood, D. W. Kurita, A. P. Lee, F. D. Lee, I. T. Lewis, F. J. Lopez, B. J. MacGowan, M. W. Poole, M. A.

- Rhodes, M. B. Schneider, N. R. Sewall, F. Y. Shimamoto, S. J. Shiromizu, D. Voloshin, A. L. Warrick, C. R. Wendland, and B. K. Young, *Rev. Sci. Instrum.*, **75**, 4177 (2004).
- [10] R. K. Kirkwood, T. Mccarville, D. H. Froula, B. Young, D. Bower, N. Sewall, C. Niemann, M. Schneider, J. Moody, G. Gregori, F. Holdener, M. Chrisp, B. J. MacGowan, S. H. Glenzer, and D. S. Montgomery, *Rev. Sci. Instrum.*, **75**, 4174 (2004).
- [11] A. J. Mackinnon, T. McCarville, K. Piston, C. Niemann, G. Jones, I. Reinbachs, R. Costa, J. Celeste, G. Holtmeier, R. Griffith, R. Kirkwood, B. MacGowan, S. H. Glenzer, and M. R. Latta, *Rev. Sci. Instrum.*, **75**, 4183 (2004).
- [12] A. J. Mackinnon, C. Niemann, K. Piston, G. Holtmeier, T. McCarville, G. Jones, I. Reinbachs, R. Costa, J. Celeste, R. Griffith, R. K. Kirkwood, B. J. MacGowan, and S. H. Glenzer, *Rev. Sci. Instrum.*, **77**, 10E529 (2006).
- [13] D. S. Montgomery and R. P. Johnson, *Rev. Sci. Instrum.*, **72**, 979 (2001).
- [14] Advanced Thin Films, 5733 Central Avenue, Boulder, CO 80301, Tel: 303-815-1545, FAX: 720-652-9948, web: <http://www.atfilms.com>.
- [15] Electro-Optics Technology, Inc., 5835 Shugart Lane, Traverse City, MI. 49684 USA, Phone: +1 231 935 4044, Fax: +1 231 935 4046, US Free: 800-697-6782, E-mail: [saleseotech.com](mailto:saleseotech.com), Web Address: [www.eotech.com](http://www.eotech.com).
- [16] R. A. London, D. H. Froula, C. M. Source, J. D. Moody, L. J. Suter, S. H. Glenzer, O. S. Jones, N. B. Meezan, and M. D. Rosen, *Rev. Sci. Instrum.*, **79**, 10F549 (2008).
- [17] P. Neumayer, C. Source, D. H. Froula, L. Divol, V. Rekow, K. Loughman, R. Knight, S. H. Glenzer, R. Bahr, and W. Seka, *Rev. Sci. Instrum.*, **79**, 10F548 (2008).
- [18] See for example: <http://www.newport.com/Pencil-Style-Calibration-Lamps/377846/1033/catalog.aspx>.